scientific reports

Check for updates

OPEN

Low dielectric properties of alkali-free aluminoborosilicate fiber glasses for PCB applications at 10 GHz

Linganna Kadathala[1], Young-Ouk Park[1], Jin-Ho Kim[2], Ji-Sun Lee[2], Jong Chan Won[3], Yun Ho Kim[3], Won-Taek Han[1] & Bok Hyeon Kim[1]✉

Alkali-free aluminoborosilicate glasses without (GDMC-Si) and with La_2O_3 addition (GDMC-La) were fabricated with an aim to develop low dielectric glass fibers for use in printed circuit boards (PCBs) as a reinforcing material in high-speed 5G/6G telecommunications application. This study presents the structural, thermo-physical, and dielectric properties of the glasses. The decrease in glass transition temperature (T_g) and the increase in coefficient of thermal expansion (CTE) were found by the addition of SiO_2 and La_2O_3 in the present glass system, which are due to the depolymerization of the glass networks confirmed by the FTIR analysis. The dielectric constants (Dk) and the dissipation factors (Df) of the glasses were investigated at a high frequency of 10 GHz. The Dk values of the GDMC-Si and GDMC-La glass systems reached a minimum of 4.50 and 4.75, while their Df values reached a minimum of 2.86×10^{-3} and 3.01×10^{-3}, respectively. Notably, the Dk and Df values of the present glasses were lower than the commercial E-glass (Dk: 6.9, Df: 7.0×10^{-3} at 10 GHz) and L-glass (Dk: 4.8, Df: 3.0×10^{-3} at 10 GHz). Glass fibers with a diameter of 10 µm were successfully drawn by the continuous melt-spinning process and their mechanical properties were investigated.

Keywords Alkali-free aluminoborosilicate glasses, Dielectric constant, Dielectric dissipation factor, Structural property, Thermomechanical property, Reinforcing material, Fiber spinning

Recently, printed circuit boards (PCBs) or printing wiring boards (PWBs) made of prepregs (PPGs) have received significant attention because of the ever-increasing demand for data transmission at higher speeds[1]. The PCBs are an essential component of electronic products and widely used in various emerging fields, including 5G/6G telecommunication, big data, internet of things (IoT), and artificial intelligence (AI) systems. PPGs are manufactured by soaking glass fiber fabrics in a polymer resin mixed with silica filler. Therefore, the performance of a PCB substrate strongly depends on the dielectric, thermal, and mechanical properties of the reinforcing glass fibers.

The dielectric loss energy (W) is determined by the Dk and Df of the PCB substrate and expressed as[2]:

$$W = K\omega v^2(Dk \cdot Df) \tag{1}$$

where K is a constant, ω is the signal frequency, and $v^2$is the potential gradient. According to the equation, the signal propagation loss increases as the Dk and Df of the glass fibers increase. As a primary reinforcement material of PCB substrates, glass fibers play an important role in the performance of PCBs because they mainly provide the benefits of mechanical strength and thermal expansion properties to the surrounding polymer resin matrix. Moreover, the critical prerequisites for the glass fibers as reinforced materials in PCB applications at higher frequencies of GHz are a low Dk (≤ 4.9), Df (≤ 0.004), softening temperature (Ts: ≤ 860 °C), and CTE (≤ 5.0 ppm/°C)[1–4]. To date, E-glass fibers are commonly used as reinforcement materials in PCB substrates owing to their moderate electrical and thermomechanical properties[4]. However, the E-glass fibers cannot be used in high-frequency applications due to its unsuitably large dielectric properties of Dk ~ 6.9 and Df ~ 0.007[4]. On the other

[1]Advanced Photonics Research Institute, Gwangju Institute of Science and Technology, 123 Cheomdangwagi-ro, Buk-gu, Gwangju 61005, Republic of Korea. [2]Display Materials Center, Korea Institute of Ceramic Engineering & Technology, Jinju 52851, Republic of Korea. [3]Division of Advanced Materials, Korea Research Institute of Chemical Technology, Daejeon 34114, Republic of Korea. ✉email: bhkim@gist.ac.kr

hand, D-glass, comprises of 72–76% SiO_2, 20–25% B_2O_3, 0–1% Al_2O_3, < 1% CaO, and < 4% $Li_2O + Na_2O + K_2O$ by weight, has a relatively low Dk of 4.1 and Df of 0.001 at 1 GHz. However, D-glass has relatively high melting and fiber forming temperatures. Thus, the global glass fiber manufacturers, such as AGY, Nittobo, and PPG, have attempted to develop alternative glass compositions with low dielectric properties that are better suited for use in PCBs for high-frequency applications[1–4]. The L-Glass by AGY, with a composition of 52–60% SiO_2, 20–30% B_2O_3, 10–18% Al_2O_3, 4–8% CaO, and < 2% F_2 by weight, has low Dk of 4.8 and Df of ~ 0.003 at 10 GHz. The NE-glass by Nittobo, which includes 50–60% SiO_2, 14–20% B_2O_3, 10–18% Al_2O_3, 1–6% MgO, 2–5% CaO, < 1% $Li_2O + Na_2O + K_2O$, and < 2% F_2 by weight, has low Dk of 4.7 and Df of ~ 0.0035 at 10 GHz. The *InnoFIBER* LD glass fiber by PPG, which comprises of 60–68% SiO_2, 7–13% B_2O_3, 9–15% Al_2O_3, 8–15% MgO, 0–4% CaO, < 2% $Li_2O + Na_2O + K_2O$, 0–1% Fe_2O_3, and 0–1% F_2 by weight, has low Dk of < 5.4 and Df of < 0.004 at 1 GHz. The presence of one or more of alkali oxides (Li_2O, Na_2O, and K_2O) in the glass fibers by the above three companies used as fluxing agents, however, cause the increase of the Df. Thus, we have tried to the develop new glass fiber compositions having lower Dk and Df values without the use of alkali oxides.

Aluminoborosilicate glasses have been commonly used in various applications including PCB substrates owing to their promising characteristics, such as excellent electrical insulation, good heat and corrosion resistance, and high thermal and mechanical stability[5–8]. Many studies have attempted to improve the thermal, mechanical, and dielectric properties of aluminoborosilicate glasses by optimizing the relative proportions of chemical constituents in the glass matrix[5–11]. Moreover, the aluminoborosilicate glasses with higher contents of SiO_2 and B_2O_3 and showed lower Dk and Df values for PCB applications[1–4,6,11,12]. Recently, the trivalent rare-earth (RE) species incorporated in small amounts as dopants were known to influence the structural, thermal, and dielectric properties of alkali-free aluminoborosilicate glasses because of their high cation field strength, which attracts the surrounding free oxygens during the formation of the glass network[6,12]. In addition, RE ions incorporated in high amounts can reduce the high-temperature viscosity of the glasses because of their role as network modifiers and their ability to create more non-bridging oxygens (NBOs)[6,12]. Moreover, they can be used for replacing the alkali and alkaline-earth oxides which generally increases the dielectric properties of the glasses. However, the dielectric properties of alkali-free aluminoborosilicate glasses, particularly at the high frequencies of 10 GHz, have not been extensively studied yet. Furthermore, to our knowledge, few studies have been found on dielectric properties of alkali-free aluminoborosilicate glasses containing high B_2O_3 content for high-frequency PCB applications.

In view of the above importance, we investigated the dielectric properties of alkali-free aluminoborosilicate glasses without and with La_2O_3 content at a high frequency of 10 GHz for PCB applications. The structural analysis of the glasses was investigated by the FTIR spectrometer. The thermal properties, such as the glass transition and onset crystallization temperatures, were studied in the glasses with respect to the SiO_2 at the expense of Al_2O_3 and La_2O_3 at the expense of Al_2O_3 and MgO. The thermomechanical properties, such as the dilatometric glass transition and softening temperatures, and the coefficient of thermal expansion, were investigated with respect to the SiO_2 and La_2O_3 contents. In addition, the spinning experiment was carried out to fabricate glass fibers for the selected glass compositions and their mechanical properties such as the tensile strength and Young's modulus were determined.

Methods

The chemical compositions of the two series of alkali-free aluminoborosilicate glasses without (referred to as GDMC-Si) and with La_2O_3 (GDMC-La) are listed in Table 1. The compositions of the GDMC-Si glasses were designed by varying the SiO_2 and Al_2O_3 contents, and the remained B_2O_3, CaO, and MgO contents were fixed at almost constant. The GDMC-La glass compositions incorporated with different contents of La_2O_3, were designed from the GDMC-Si59 glass composition referred as a reference glass. The glasses were fabricated using the melt-quenching method. Raw materials used for the fabrication of glasses were high purity powders of SiO_2, Al_2O_3, B_2O_3, $MgCO_3$, $CaCO_3$, and La_2O_3 (Kojundo, Japan, ≥99.9%). The batch materials were pulverized using a ball mill for 2 h and the homogeneous batch powders were taken into an alumina crucible and melted in an electric furnace. Before melting the batch compositions at elevated temperature, the following two steps were carried out in the melting process: (1) Dehydration of the batch chemical constituents at 200 °C for the removal of moisture water and (2) Decarbonization in the range of 800–900 °C for the removal of carbonates. Then, the batches were melted at 1650 °C for the duration of 3 h using an electric furnace. The molten glasses were then cast onto a pre-heated brass plate at 650 °C; it was then annealed at 650 °C for 2 h to release the residual stress

Glass label	Chemical composition (mol%)						Composition ratio	
	SiO_2	Al_2O_3	B_2O_3	CaO	MgO	La_2O_3	SiO_2/Al_2O_3	$La_2O_3/(Al_2O_3+MgO)$
GDMC-Si59	59.5	10.20	19.6	5.5	5.20	0	5.83	-
GDMC-Si61	61.1	8.80	19.4	5.5	5.20	0	6.94	-
GDMC-Si62	62.7	7.40	19.2	5.5	5.20	0	8.47	-
GDMC-La0.2	59.5	10.07	19.6	5.5	5.13	0.2	-	0.013
GDMC-La0.4	59.5	9.93	19.6	5.5	5.07	0.4	-	0.026
GDMC-La0.8	59.5	9.67	19.6	5.5	4.93	0.8	-	0.055
GDMC-La1.2	59.5	9.40	19.6	5.5	4.80	1.2	-	0.084

Table 1. Chemical compositions of the alkali-free aluminoborosilicate glasses.

and cooled to 25 °C. Finally, the glass samples were cut into 85 × 85 mm^2 size and polished to the thickness of 0.78 mm to characterize their dielectric properties.

We selected two glass compositions, GDMC-Si59 and GDMC-La0.2 with a size of 65 × 65 × 10 mm^3 to draw glass fibers by using the spinning process. The thermal stability (ΔT) of these two glasses was found to be ≥ 224 °C, conferring them enough stability against crystallization during the fiber spinning process. Successfully, the glass fibers with a total length of 25 km and diameter of about 10 µm were obtained by the continuous melting spinning process at 1380 °C for the duration of 100 minutes at a spinning speed of 500 rpm using the glass pieces with a total weight of about 800 g. The detailed fiber spinning process was discussed later.

The densities of the glasses were measured by a densimeter (Alfa Mirage, MD-300 S). Each glass sample was measured at least thrice and the measurement errors of the density were within ±0.003 g/cm^3. The infrared absorption spectra of the glasses were measured using an attenuated total reflection-FTIR spectrometer (Bruker, ATR-FTIR Vertex 70v) in the frequency range of 550–1800 cm^{-1} with a step of 2 cm^{-1}.

The differential thermal analysis (DTA) curves of the glasses were obtained in the temperature range of 25–1400 °C using a Netzsch STA 409 apparatus at a scan rate of 10 °C/min. The thermomechnical analysis (TMA) curves of the glasses were obtained in the temperature range of -10 to 900 °C using a Netzsch TMA 402 C apparatus at a scan rate of 5 °C/min in an N_2 flowing atmosphere. Glass samples of size 5 × 5 × 10 mm^3 were used for the TMA measurements.

The dielectric properties of the glasses, namely the Dk and Df values, were measured at higher frequencies of 10 GHz and 28 GHz using two techniques of the split-post dielectric resonator (QWED, SPDR) and the Fabry–Pérot open resonator (QWED, FPOR) together with a vector network analyzer (VNA, Anritsu, MS4647B). Additionally, the cavity resonator (Anritsu) with a VNA (Keysight, E5080B) was used for measurements at 40 GHz. The measurement accuracy of the Dk and Df values was within 0.5% and 2%, respectively. Polished thin glass sheets of dimensions 85 × 85 × 0.78 mm^3 were used for the measurements.

Results and discussion

Figure 1(A) depicts the FTIR spectra of the GDMC-Si glasses with different concentrations of SiO_2 substituted for Al_2O_3 in the range of 550–1800 cm^{-1}, where the three frequency bands appeared similarly for all the investigated glasses. The low-, middle-, and high-frequency absorption bands, were shown in the ranges of 570−800, 850−1250, and 1250–1600 cm^{-1}, respectively. The low-frequency absorption bands, peaking at approximately 572 and 604 cm^{-1}, can be attributed to the vibrations of the Si−O−Si and Al−O−Al bonds[5–8,11–15]. The absorption bands at approximately 664 and 787 cm^{-1} can be assigned to the vibration modes of the B-O related groups, namely the borate, borate rings, and boroxol rings[5–8,11–15]. The absorption bands appeared at approximately 899 (Q^1), 1024 ([SiO_4] tetrahedral units), and 1142 cm^{-1} (Q^4), correspond to the Si−O_{nb} and Si−O_b stretching vibrations of the [SiO_4] tetrahedral units, respectively. But the Q^2 and Q^3 units were not appeared in the GDMC-Si glasses. Note that the [SiO_4] tetrahedral units are represented using the Q^n notation, where n denotes the number of bridging oxygens coordinated to the silicate tetrahedra ($n = 1, 2, 3$, and 4)[5–8,11–15]. The high-frequency absorption band appearing at approximately 1377 cm^{-1} is attributed to the stretching vibrations of the B-O bonds in the [BO_3] triangles[5–8,11–15].

Figure 1(B) shows the normalized FTIR spectra of the GDMC-Si glasses shown in Fig. 1(A). The spectra were normalized at the low frequency band located at ~664 cm^{-1} to well disclose the changes of the broad absorption band appeared in the range of 850–1250 cm^{-1}. It can be noted that the observed absorption bands are broad and overlapped due to strong SiO_2 and B_2O_3 structural unit vibrations. Therefore, the absorption bands were de-convoluted using a Gaussian function to identify each component peak in the FTIR spectrum (Fig. 1(C) and (D)). The peak positions, peak areas, and full-widths at half maxima (FWHMs) of the de-convoluted peaks are summarized in Table 2.

The absorption bands around 899 and 1021 cm^{-1} shifted to lower wavenumbers, and the absorption intensities increased at 899 cm^{-1} and decreased at 1021 cm^{-1} with increasing substitutions of SiO_2 for Al_2O_3, resulting from the depolymerization of the silicate glass network (Fig. 1(B)). The absorption band intensities at approximately 787 and 1377 cm^{-1} corresponding to the vibration modes of the B-O bonds continuously increased for the bands with the increase in SiO_2 substitution for Al_2O_3 in the GDMC-Si glass system. Considering the relative areas of the absorption bands as shown in Table 2, the structural changes in the GDMC-Si glasses with the increase of SiO_2/Al_2O_3 ratio can be explained. The relative areas of the deconvoluted peaks located at ~ 1021 cm^{-1} (SiO_4) decreased from 65 to 58%, ~ 899 cm^{-1} (Q^1) increased from 23 to 26%, and ~ 1139 cm^{-1} (Q^4) increased from 14 to 15%. These results reveal that the glass network connectivity decreased with the increase of SiO_2/Al_2O_3 ratio in the GDMC-Si glass system because of the dominance of the non-bridging Q^1 units. Structural changes have been reported in the aluminoborosilicate glasses upon the substitution of Al_2O_3 for SiO_2[11,14]. Junfeng et al[11]. reported that by substituting the Al_2O_3 for SiO_2, the stretching vibrational modes of the Si-O_b bonds increased due to the enhancement of the [AlO_4] tetrahedron in the glass network structure. In the alkali-free aluminoborosilicate glasses, most of the Al^{3+} ions exist in the form of [AlO_4]$^-$ tetrahedra when the (MgO + CaO)/Al_2O_3ratio is greater than 1[11]. In this glass system, the alkaline-earth cations (R^{2+}: Ca^{2+}, Mg^{2+}) compensate the [AlO_4]$^-$ tetrahedral units with the increase of the Al_2O_3content, leading to a more polymerized network structure. Bruns et al[14]. also reported that the Si−O−Al bonds connectivity was enriched with the addition of Al_2O_3 for SiO_2 in borosilicate glasses. In the present study, the glass network is depolymerized with the substitution of SiO_2 for Al_2O_3 because of the excess R^{2+} ions prefer to form NBOs rather than to compensate the negatively charged [BO_4]$^-$ tetrahedral units.

Figure 2(A) shows the FTIR spectra of the GDMC-La glasses with different concentrations of La_2O_3 substituted for Al_2O_3 and MgO. Figure 2(B) shows the normalized FTIR spectra of the GDMC-La glasses. As shown in the figure, similar absorption bands were observed at slightly different peak positions in comparison to those of the GDMC-Si glasses. The peak positions, peak areas, and FWHM of the de-convoluted absorption

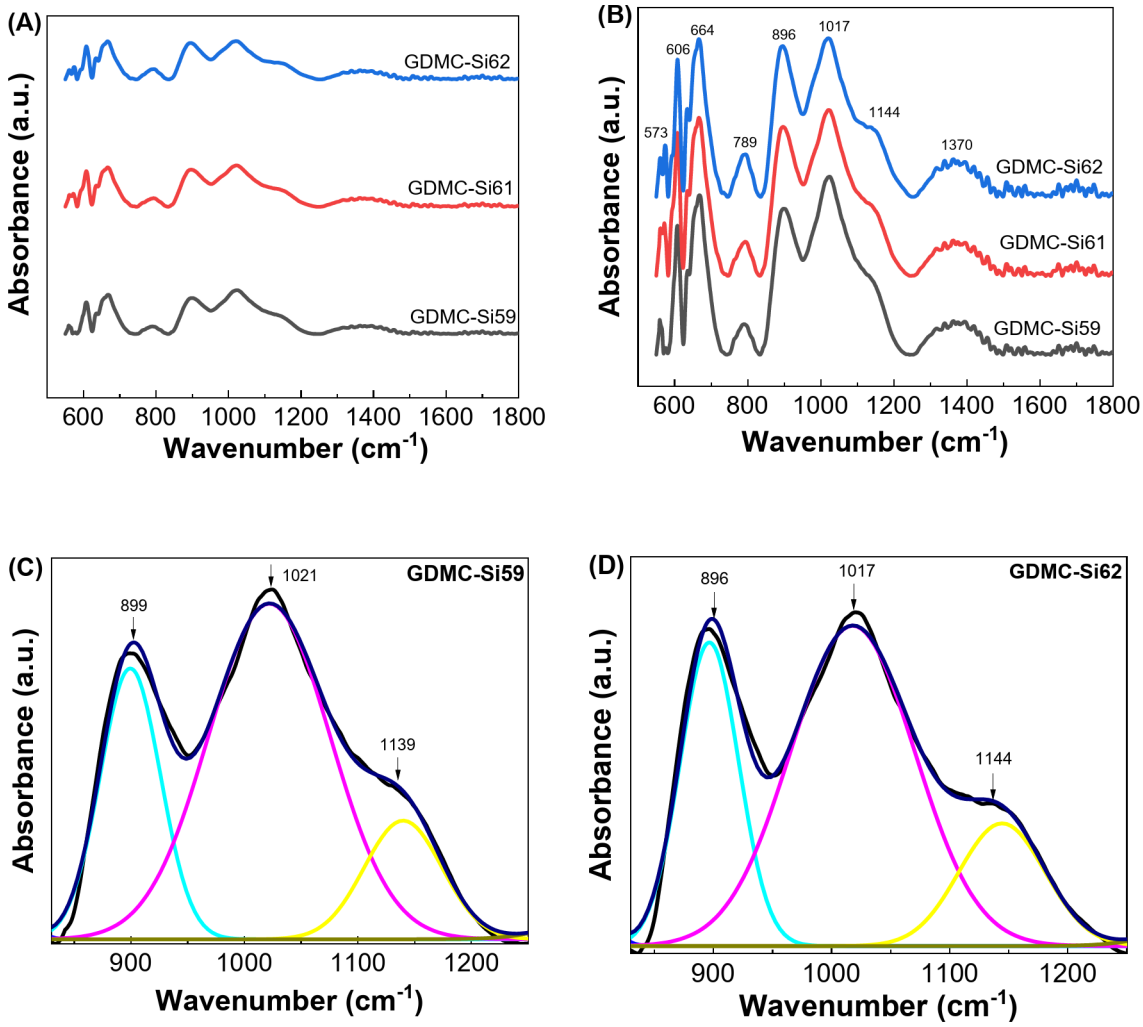

Fig. 1. FTIR spectra of the GDMC-Si glasses with different SiO_2 contents (**A**) before and (**B**) after the normalization. Deconvolution of the FTIR bands for the (**C**) GDMC-Si59 and (**D**) GDMC-Si62 glasses.

Item	Infrared bands (cm^{-1})		
	Q^1	$[SiO_4]$	Q^4
GDMC-Si59			
Peak position	899	1021	1139
Area	57.52(24.6%)	143.47(61.5%)	32.44(13.9%)
FWHM	62.66	126.07	80.62
GDMC-Si61			
Peak position	897	1019	1143
Area	56.48(25.5%)	135.16(61.0%)	29.8(13.4%)
FWHM	60.96	128.70	81.00
GDMC-Si62			
Peak position	896	1017	1144
Area	55.73(26.1%)	124.48(58.4%)	32.94(15.4%)
FWHM	58.57	123.95	85.67

Table 2. FTIR bands, peak positions, peak areas, and full widths at half maxima (FWHMs) of the GDMC-Si glasses. The relative areas of the deconvoluted peaks are shown in parentheses.

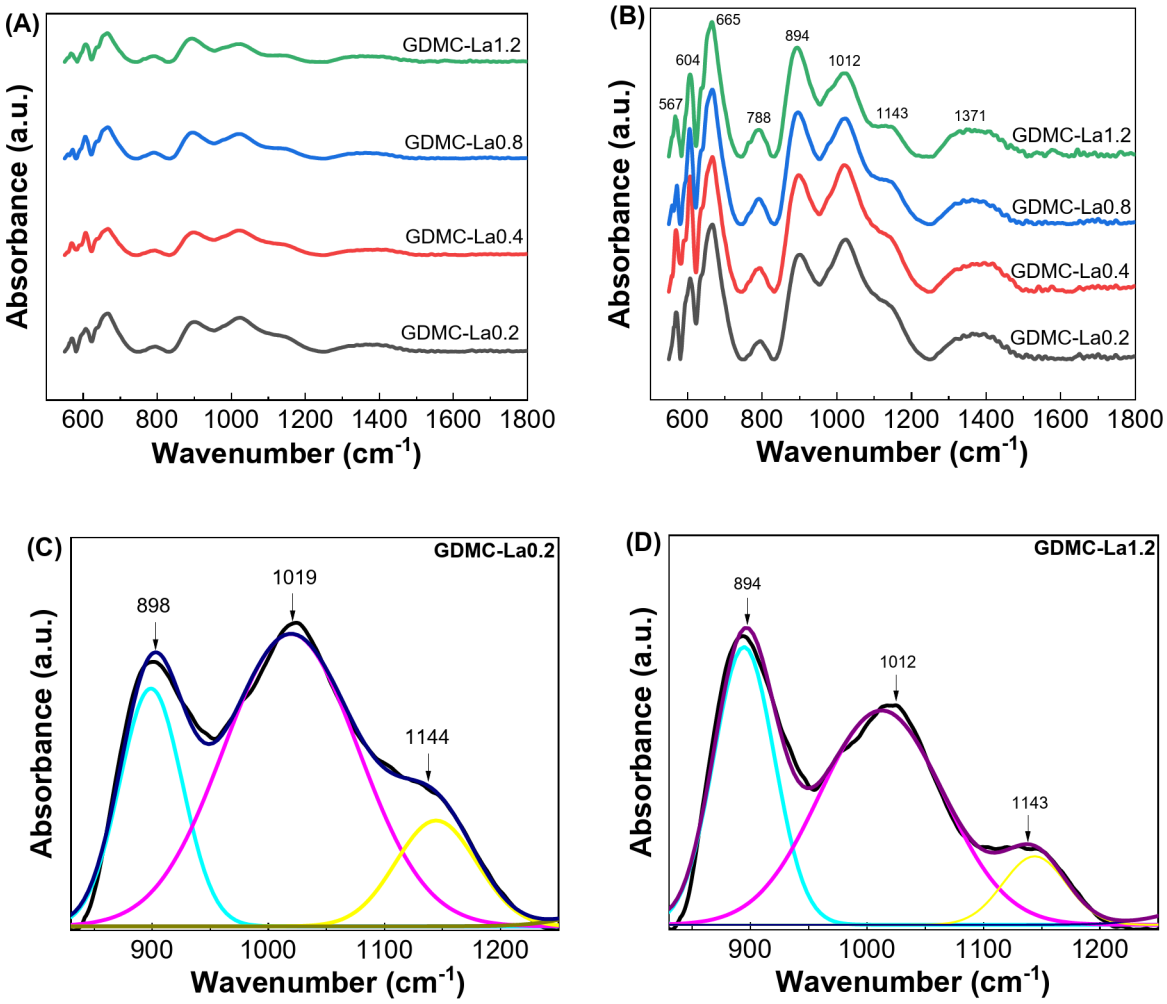

Fig. 2. (A) FTIR spectra of the GDMC-La glasses for different La_2O_3 contents (**A**) before and (**B**) after the normalization. Deconvolution of the FTIR bands for the (**C**) GDMC-La0.2 and (**D**) GDMC-La1.2 glasses.

bands are listed in Table 3. The deconvoluted FTIR spectra of the GDMC-La0.2 and the GDMC-La1.2 glasses are shown in Fig. 2(C) and (D), respectively. The absorption band at 1019 cm^{-1} corresponding to the stretching vibrations of the bridging Si-O_b bonds in the [SiO_4] units, shifted to a lower wavenumber of 1012 cm^{-1}, and the absorption intensity steadily decreased with the increase of La_2O_3 content. The absorption band at 898 cm^{-1} corresponding to the vibrations of the Si-O_{nb} bonds (Q^1) in the [SiO_4] tetrahedral units, shifted to a lower wavenumber of 894 cm^{-1}, and the absorption intensity progressively increased with the increase of La_2O_3 content. The absorption intensity of the band at 1144 cm^{-1} (Q^4) steadily decreased with the increase of La_2O_3 content. Notably, the absorption band intensity at 898 cm^{-1} becomes dominated at a high concentration of La_2O_3 (> 0.4 mol%) in comparison with the absorption band at 1019 cm^{-1}. The relative areas of the deconvoluted peaks located at ~ 1019 cm^{-1} (SiO_4) decreased from 63 to 56%, ~ 898 cm^{-1} (Q^1) increased from 24 to 35%, and ~ 1144 cm^{-1} (Q^4) decreased from 14 to 9% with the increase of La_2O_3 content from 0.2 to 1.2 mol%. The increase in the absorption band intensity of the Si-O_{nb} bonds around 898 cm^{-1} and the decrease in the absorption band intensity of the Si-O_b bonds around 1019 and 1144 cm^{-1} support that the glass network becomes loosened with increasing La_2O_3concentration in the GDMC-La glass system because of the increase of the NBOs in the glass network structure[6,12].

Results from the FTIR spectral analysis, plus T_g and CTE (will be discussed later) demonstrated that the glass network of the both glass systems was depolymerized with the increase of SiO_2 at the expense of Al_2O_3 and La_2O_3 at the expense of Al_2O_3 and MgO.

As a macroscopic physical parameter, the density depends on the glass composition, degree of polymerization, and the coordination number of the atoms. Figure 3 shows the variations in density with respect to the SiO_2/Al_2O_3 and La_2O_3/(Al_2O_3 + MgO) ratios in the GDMC-Si and the GDMC-La glasses. As shown in Fig. 3(A), the density continuously decreased in the range of 2.346–2.311 g/cm^3 with the increase of the SiO_2/Al_2O_3 ratio from 5.8 to 8.4 in the GDMC-Si glasses. This trend is attributed to the lighter molar mass of SiO_2 (60.08 g/mol) compared with that of Al_2O_3 (101.96 g/mol), indicating a loosened glass structure with the increase of the SiO_2/Al_2O_3 ratio. At the same time, the density showed a linear increase in the range of 2.375–2.449 g/cm^3 with the increase of La_2O_3/(Al_2O_3 + MgO) ratio from 0.013 to 0.084 for the GDMC-La glasses as shown in Fig. 3(B). The

Item	Infrared bands (cm^{-1})		
	Q^1	[SiO_4]	Q^4
GDMC-La0.2			
Peak position	898	1019	1144
Area	46.29(23.7%)	122.67(62.7%)	26.65(13.6%)
FWHM	63.46	136.68	82.06
GDMC-La0.4			
Peak position	897	1018	1143
Area	51.64(25.2%)	126.77(62.0%)	26.02(12.7%)
FWHM	62.88	134.39	79.30
GDMC-La0.8			
Peak position	896	1015	1144
Area	50.23(28.8%)	102.77(59.0%)	21.18(12.2%)
FWHM	61.54	129.43	76.24
GDMC-La1.2			
Peak position	894	1012	1143
Area	49.75(35.2%)	78.63(55.8%)	12.66(8.9%)
FWHM	61.19	125.58	63.52

Table 3. FTIR bands, peak positions, peak areas, and FWHMs in the GDMC-La glasses. The relative areas of the bands are shown in parentheses.

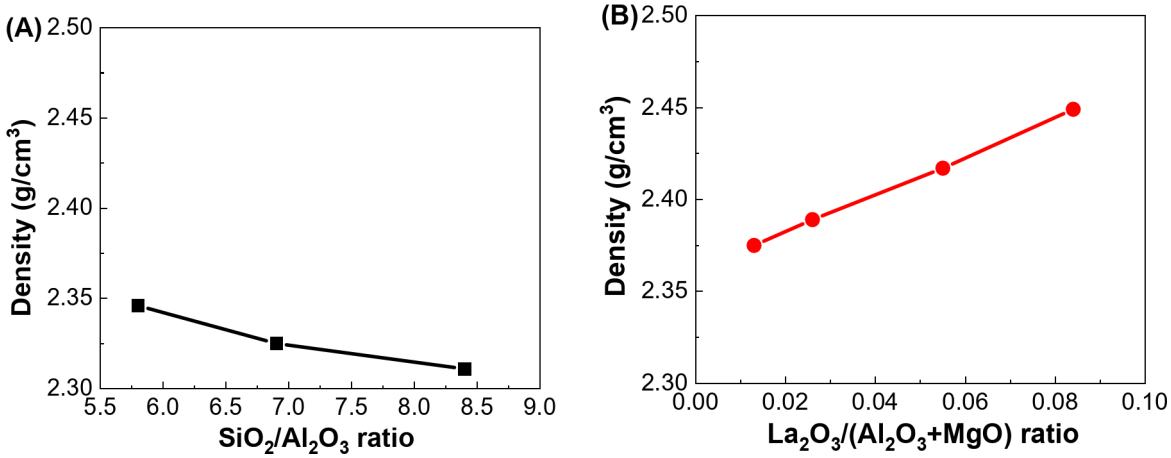

Fig. 3. Variation trend in the densities with respect to the (**A**) SiO_2/Al_2O_3 and (**B**) $La_2O_3/(Al_2O_3+MgO)$ ratios in the GDMC-Si and the GDMC-La glasses.

observed density trend is attributed to the heavier molar mass of La_2O_3 (325.81 g/mol) compared with that of Al_2O_3 (101.96 g/mol). It is noted that the GDMC-Si and the GDMC-La glass systems have a lower density by approximately 10–12% and 9 − 6%, respectively, compared to the E-glass ($\rho = 2.59$ g/cm^3). The improvement in density is desirable for high-speed PCBs, which require reinforced glass fiber with lighter weight.

Investigation on the thermal characteristics of glasses is essential to confirm their crystallization-resistance for PCB applications. Glass should be thermally stable when subjected to thermal treatment during the fiber-spinning process. Thus, we performed thermal characterization of the studied glasses to determine their thermal stability. Figure 4(A) and (B) show the DTA curves of the glasses in the temperature range of 400–1200 °C. From the curves, the endothermic and exothermic events, such as the glass transformation (T_g) and crystallization (T_x) temperatures were examined. The T_g and T_x values were obtained from the onset points of the endothermic and exothermic events in the measured DTA curves, respectively. The quantitative T_g, T_x, and ΔT values of the two glass systems are shown in Fig. 4(C) and (D) and Table 4.

As the SiO_2/Al_2O_3 ratio increased from 5.8 to 8.4 in the GDMC-Si glasses, the T_g slightly decreased from 686 to 681 °C and the T_x were in the range of 908–922 °C. The T_g of the GDMC-La glasses decreased from 690 to 681 °C, while the T_x increased from 918 to 931 °C with the increase of the $La_2O_3/(Al_2O_3+MgO)$ ratio from 0.013 to 0.084. The T_g is known to be governed by the network connectivity and the introduction of NBOs into a silicate network thus generally decreases T_g[6,15]. The T_g trends observed for the GDMC-Si and the GDMC-La glasses suggest that the NBOs increased with the increase of the SiO_2/Al_2O_3 and $La_2O_3/(Al_2O_3+MgO)$ ratios, which is consistent with the FTIR analysis. The ΔT of the glasses was also examined from the obtained T_g and T_x. The

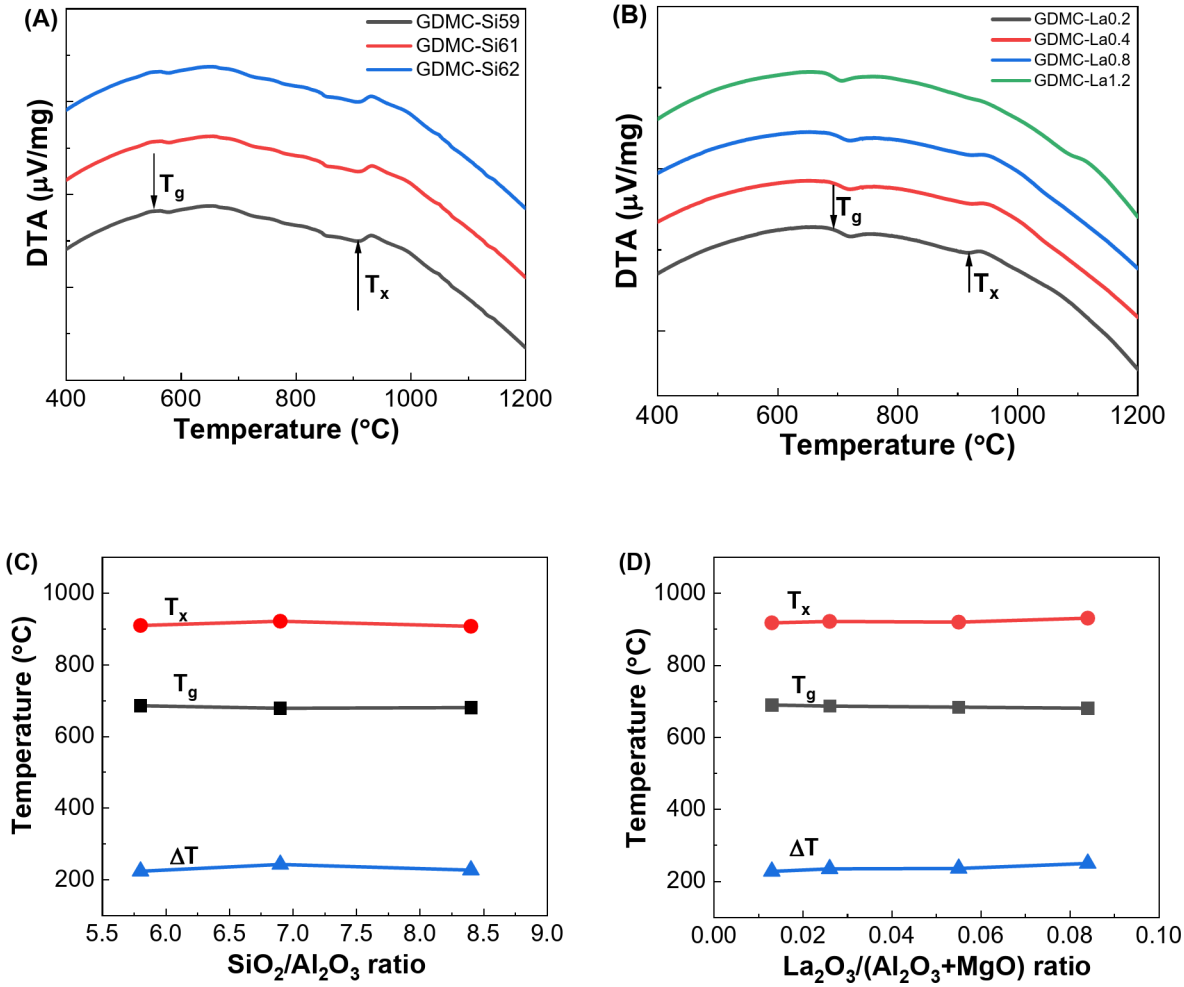

Fig. 4. (**A**, **B**) DTA curves and (**C**, **D**) quantitative values of the glass transformation temperatures (T_g), glass crystallization temperatures (T_x), and thermal stabilities ($\Delta T = T_g - T_x$) of the GDMC-Si and the GDMC-La glass systems.

Glass label	T_g (°C)	T_x (°C)	ΔT (°C)
GDMC-Si59	686	910	224
GDMC-Si61	679	922	243
GDMC-Si62	681	908	227
GDMC-La0.2	690	918	228
GDMC-La0.4	687	922	235
GDMC-La0.8	684	920	236
GDMC-La1.2	681	931	250

Table 4. Quantitative glass transformation temperature (T_g), glass crystallization temperatures (T_x) and thermal stability (ΔT) in the alkali-free aluminoborosilicate glasses.

ΔT should be ≥ 100 °C to minimize the possibility of devitrification during the glass-fiber spinning process[7]. All glasses showed good ΔT that exceeded 224 °C, which indicates that the GDMC-Si and the GDMC-La glasses in this study have enough stability against devitrification. Notably, the GDMC-La glasses showed higher thermal stability than that of the reference glass (GDMC-Si59), ensuring the feasibility for fiber spinning.

TMA curves of the GDMC-Si and the GDMC-La glasses were measured to investigate the thermomechanical properties, such as the dilatometric glass transition temperature (T_{dg}), dilatometric softening temperature (T_{ds}), and coefficient of thermal expansion (CTE). Figure 5(A) and (B) depict the TMA curves of the GDMC-Si and the GDMC-La glasses, respectively. Characteristic properties, such as the T_{dg}, T_{ds}, and CTE, were determined from the TMA curves and listed in Table 5. Figure 5(C) and (D) show the quantitative T_{dg}, T_{ds}, and CTE values with respect to the SiO_2/Al_2O_3 and $La_2O_3/(Al_2O_3+MgO)$ ratios in the GDMC-Si and the GDMC-La glass

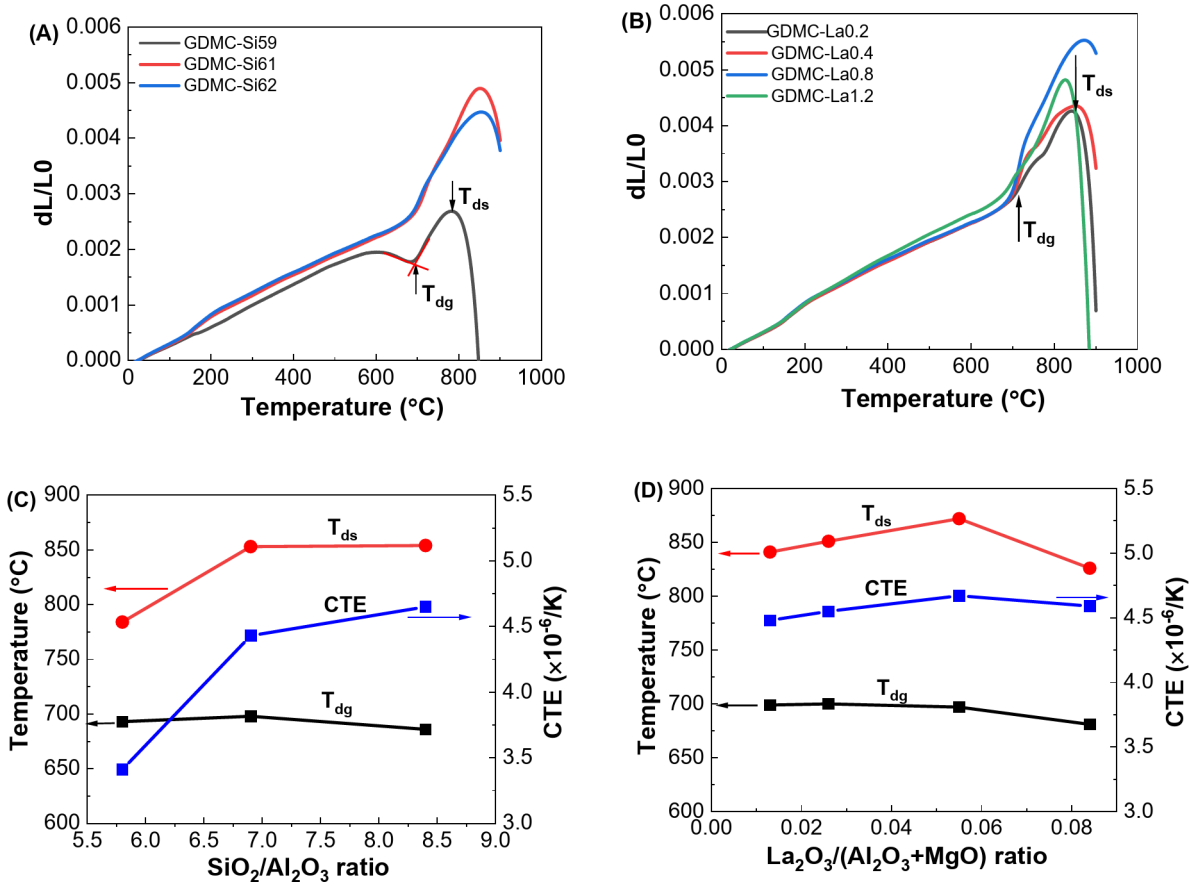

Fig. 5. (**A**, **B**) Thermomechanical curves and (**C**, **D**) quantitative values of the dilatometric glass transition temperatures (T_{dg}), dilatometric glass softening temperatures (T_{ds}), and coefficients of thermal expansion (CTE) in the GDMC-Si and the GDMC-La glasses.

Glass label	T_{dg} (°C)	T_{ds} (°C)	CTE ($\times 10^{-6}$/K)	Reference
GDMC-Si59	693	784	3.41	This work
GDMC-Si61	698	853	4.43	
GDMC-Si62	686	854	4.65	
GDMC-La0.2	699	841	4.48	
GDMC-La0.4	700	851	4.55	This work
GDMC-La0.8	697	872	4.67	
GDMC-La1.2	681	826	4.59	
E-glass	-	846	5.4	[4]
NE-glass	-	-	3.3	[16]
AGY L-glass	-	850	3.9	[17]

Table 5. Quantitative dilatometric glass transition temperature (T_{dg}), dilatometric glass softening temperature (T_{ds}), and coefficient of thermal expansion (CTE) values of the alkali-free aluminoborosilicate glasses.

systems, respectively. The onset point, which is the temperature corresponding to the intersection of the two linear parts with different slopes, was used to represent the T_{dg}. The T_{dg} of the GDMC-Si glasses were in the range of 693–686 °C and were close to those obtained from the STA measurement. The T_{ds} of the glasses were in the range of 784–854 °C. The T_{dg} decreased and the T_{ds} increased with the increase of the SiO_2/Al_2O_3 ratio from 5.8 to 8.4. The T_{dg} and T_{ds} of the GDMC-La glasses were in the range of 699–681 °C and 872–826 °C with the increase of the $La_2O_3/(Al_2O_3+MgO)$ ratio from 0.013 to 0.084. The T_{dg} decreased from 699 to 681 °C with the increase of the $La_2O_3/(Al_2O_3+MgO)$ ratio from 0.013 to 0.084, while the T_{ds} increased from 841 to 872 °C with increasing ratio up to 0.055 and then decreased to 826 °C for further increase in the ratio of 0.084. The CTE was obtained by linear fitting of the curves in the temperature region between 25 and 200 °C. The CTE of the

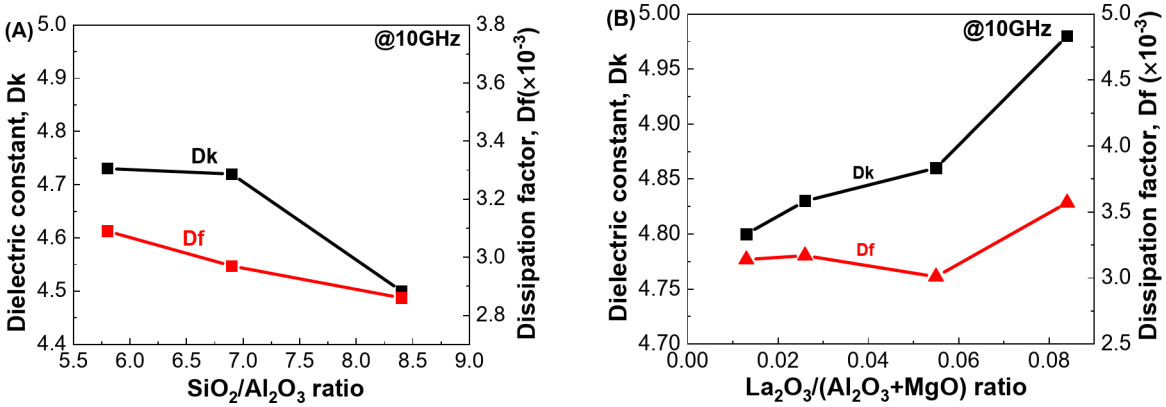

Fig. 6. Dielectric properties (Dk, Df) of the (**A**) GDMC-Si and (**B**) GDMC-La glasses.

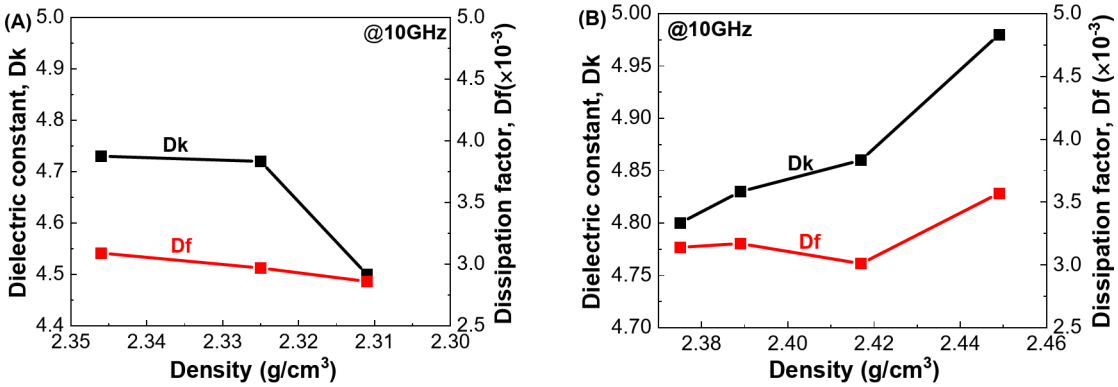

Fig. 7. Variations of the dielectric constant (Dk) and dielectric dissipation factor (Df) with respect to the glass densities in the (**A**) GDMC-Si and (**B**) GDMC-La glasses.

GDMC-Si glasses increased from 3.41 to 4.65 ($\times 10^{-6}$/K) with the increase of SiO_2/Al_2O_3 ratio from 5.8 to 8.4, respectively. The CTE of the GDMC-La glasses were in the range of 4.48–4.67 ($\times 10^{-6}$/K) with the increase of $La_2O_3/(Al_2O_3 + MgO)$ ratio from 0.013 to 0.084. The decrease in T_{dg} and the increase in CTE with the increase of the SiO_2 at the expense of Al_2O_3 or La_2O_3 at the expense of $(Al_2O_3 + MgO)$ in the studied glasses are caused by the depolymerization of the silicate glass network. The variations in the T_{dg}, T_{ds}, and CTE within the investigated compositional range are consistent with the changes observed in the FTIR spectra. The T_{ds} and of the present glasses are compatible with those of commercially available glasses, such as E-[4], NE-[16], and AGY L-glasses[17]. These low T_{ds} and CTE values indicate that the GDMC-Si and the GDMC-La glass systems are applicable for the development of PCB substrates.

Figure 6(A) shows the dielectric properties of the GDMC-Si glasses with respect to the SiO_2/Al_2O_3 ratio at a frequency of 10 GHz. The Dk and the Df of the GDMC-Si glasses at a frequency of 10 GHz were in the range of 4.73–4.50 and 3.09–2.86 ($\times 10^{-3}$), respectively. Figure 6(B) shows the dielectric properties of the GDMC-La glasses with different $La_2O_3/(Al_2O_3 + MgO)$ ratios. The Dk and the Df at a frequency of 10 GHz for the GDMC-La glasses were in the range of 4.80–4.98 and 3.14–3.57 ($\times 10^{-3}$), respectively. As shown in Fig. 6(A), the Dk and the Df decreased from 4.73 to 4.50 and 3.09 to 2.86 ($\times 10^{-3}$) with the increase of the SiO_2/Al_2O_3 ratio from 5.8 to 8.4, respectively. For the GDMC-La glass system, the Dk increased from 4.80 to 4.98 and the Df were in the range of 3.14–3.57 ($\times 10^{-3}$) with the increase of $La_2O_3/(Al_2O_3 + MgO)$ ratio from 0.013 to 0.084, as shown in Fig. 6(B).

According to the well-known Clausius-Mossotti (CM) equation[18], the Dk depends on the glass density and the polarizability of the glass constituents. The density of the glasses decreased with the substitution of SiO_2 for Al_2O_3, resulting in the decrease of the Dk, as shown in Fig. 7(A). Conversely, the density of the GDMC-La glasses increased with the increase of La_2O_3, resulting in the increase of the Dk, as shown in Fig. 7(B). In addition, the polarizability of the glass constituents plays an important role in their dielectric properties[18]. The polarizability of Si^{4+} (0.033Å^3) is lower than that of the substituted Al^{3+} (0.054Å^3)[19]. Thus, the GDMC-Si glasses with increased SiO_2 contents are expected to have lower polarizabilities and this contributed to the decrease of Dk in the glasses. Similarly, the increase of Dk in the GDMC-La glasses may be explained by considering the polarizability. The Dk increased with the increase of La_2O_3 substituting for Al_2O_3 and MgO in the GDMC-La glasses can be attributed to the high polarizability of La^{3+} (1.052 Å^3) compared with those of Al^{3+} (0.054Å) and Mg^{2+}(0.094Å)[19–21].

The dielectric polarizability (α_D) of the GDMC-Si and the GDMC-La glasses was estimated using the CM equation shown below:

$$\alpha_D = \left(\frac{3V_m}{4\pi N_A}\right)\left[\frac{Dk-1}{Dk+2}\right] \quad (2)$$

where V_m is the molar volume and N_A is the Avogadro number (6.023×10^{23} mol^{-1}). The α_D values of the GDMC-Si glasses were found to decrease from 6.08 to 5.88 $Å^3$ with increasing SiO_2 content from 59.5 to 62.7 mol%, respectively. The α_D values of the GDMC-La glasses were found to increase from 6.10 to 6.26 $Å^3$ with increasing La_2O_3 content from 0.2 to 1.2 mol%, respectively. This explains that the Dk decreased with increasing SiO_2 and increased with increasing La_2O_3 are attributed to the decrease and the increase of α_D in the GDMC-Si and GDMC-La glasses, respectively.

The Df of glasses is influenced by ion migration and network connectivity properties[5–8,22,23]. At lower frequencies (< 1 GHz), the ion migration contributes to the Df[5–8], whereas at higher frequencies (> 1 GHz), the Df is mainly influenced by the network losses[22,23]. The Df of the GDMC-Si glasses decreased upon the substitution of SiO_2 for Al_2O_3. Such a decrease in the Df is attributed to the more covalent $[SiO_4]$ tetrahedra that replacing the more ionic $[AlO_4]^-$ tetrahedra. As a result, the Df decreases, because in covalent bonds the electron density is more evenly distributed between two atoms. Therefore, the displacement of ions in the glass network is expected to be less pronounced by an external electromagnetic field. Furthermore, the decrease of Df may be due to the dominance of the three-fold boron $[BO_3]$, which is less polarizable when compared to the four-fold $[BO_4]$ as confirmed from the FTIR spectra in the GDMC-Si glasses. The Df of the GDMC-La glasses decreased with the substitution of La_2O_3 for Al_2O_3 and MgO up to 0.8 mol% may be attributed to a higher coordination environment of La^{3+} ions in the glass network. In addition, the larger atomic weight of La_2O_3reduced the motion of the mobile ions, resulting in the decrease of the Df[6,12]. Moreover, the Df decreases with the increase of La_2O_3 as a result of an increase of NBOs which reduces the R^{2+} (R = Mg, Ca) ions mobility in the glass network. However, the microscopic origin of Df in the multicomponent glasses at GHz frequency range is to be more explored.

The Dk and the Df of the GDMC-Si and the GDMC-La glass systems along with the reported commercial glasses are shown in Table 6. The Dk values of the GDMC-Si and the GDMC-La glass systems reached a minimum of 4.50 and 4.75, respectively, while their Df values reached a minimum of 2.86×10^{-3} and 3.01×10^{-3}. Notably, the present glasses showed lower Dk and Df values than those of the commercial E-glass (Dk: 6.9, Df: 7.0×10^{-3} at 10 GHz), L-glass (Dk: 4.8, Df: 3.0×10^{-3} at 10 GHz), NE-glass (Dk: 4.7, Df: 3.5×10^{-3} at 10 GHz), and *InnoFIBER* LD (Dk: < 5.4, Df: 4.0×10^{-3}at 1 GHz)[1–4,16,17]. The characterization of glasses in the mm-wave region (> 10 GHz) is of great interest for 5th generation of mobile communications[22]. Table 6presents the Dk and the Df values of the GDMC-Si59 and the GDMC-La0.2 glasses measured at higher frequencies of 28 GHz and 40 GHz. The measurement results show that the Dk decreased and the Df increased with increasing frequency in the range of 10 to 40 GHz for both the glasses, which are consistent with the reported characteristics in the literature[22,23]. The decrease in Dk with frequency may be due to the decrease of polarizability that is caused by the phase lag between the dipole alignment and the electric field as the frequency increases[22,23]. The trend of Df with frequency can be attributed to the network losses that originated from the movements of parts of the glass network structure[22,23].

Figure 8(A) and (B) show the schematic diagram of continuous fiber spinning process and the photograph of the fiber spinning equipment, respectively, consisting of 10 nozzle bushing, binder roller, winder, and temperature controller. As stated before in relation to the DTA data, since the thermal stability of ΔT was large ≥ 224 °C, both series of glasses was expected to be stable enough against crystallization during the fiber spinning process at high temperature of 1380 °C. We selected two glass compositions, the GDMC-Si59 and the GDMC-La0.2 with a size of $65\times65\times10$ mm^3 and about 800 g weight each (Fig. 8(C)) for fiber spinning process. Melting and spinning was carried out at the same time. Firstly, the glass slab was melt in the bushing by increasing temperature successively from 1350 °C (42 min), 1370 °C (15 min), to 1380 °C (13 min) to obtain a homogenized melt. Then, the melt was allowed to drop from the 10 bushing nozzles with each hole size of $\phi1.5\times3$ mm^2 (Fig. 8(D)). Finally, the 10 glass fibers were drawn through the nozzles at 1380 °C for the duration of 100 min and the 10 fibers were combined to one fiber strand. Then, the fiber strand was collected by winding it on a spool with a diameter of 155 mm at a

	at 10 GHz		at 28 GHz		at 40 GHz		
Glass label	Dk	Df ($\times10^{-3}$)	Dk	Df ($\times10^{-3}$)	Dk	Df ($\times10^{-3}$)	Reference
GDMC-Si59	4.73	3.09	4.70	4.40	4.64	4.78	This work
GDMC-Si61	4.72	2.97	-	-	-	-	
GDMC-Si62	4.50	2.86	-	-	-	-	
GDMC-La0.2	4.80	3.14	4.81	4.56	4.78	4.76	This work
GDMC-La0.4	4.83	3.17	-	-	-	-	
GDMC-La0.8	4.86	3.01	-	-	-	-	
GDMC-La1.2	4.98	3.57	-	-	-	-	
E-glass	6.90	7.00	-	-	-	-	1–4
NE-glass	4.70	3.50	-	-	-	-	1–4,16
AGY L-glass	4.80	3.00	-	-	-	-	1–4,17

Table 6. Dielectric constants (Dk) and dissipation factors (Df) of the alkali-free aluminoborosilicate glasses at 10, 28, and 40 GHz.

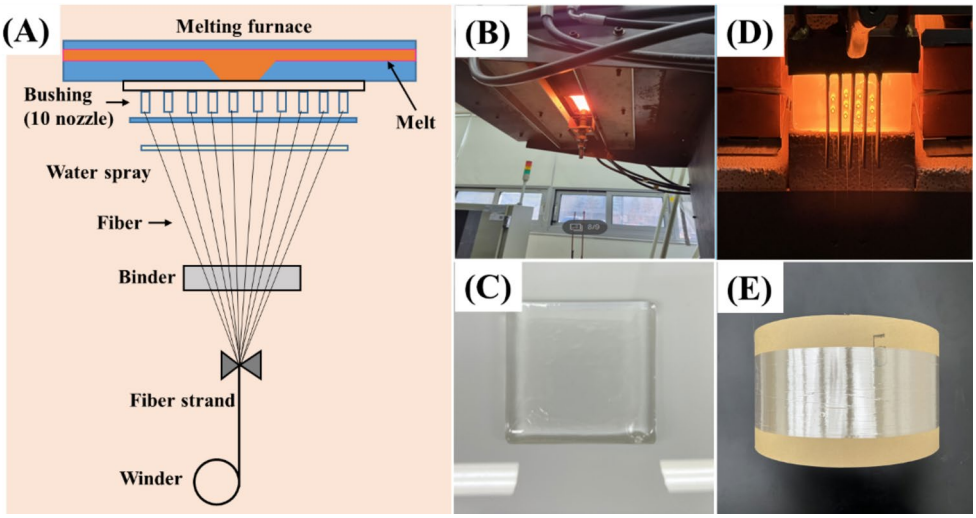

Fig. 8. (**A**) Schematic diagram of continuous fiber spinning process; Photographs of the (**B**) continuous melting spinning equipment, (**C**) bulk glass sample; (**D**) drawing of the glass melt from the bushing nozzle, and (**E**) the fiber strands on the spool.

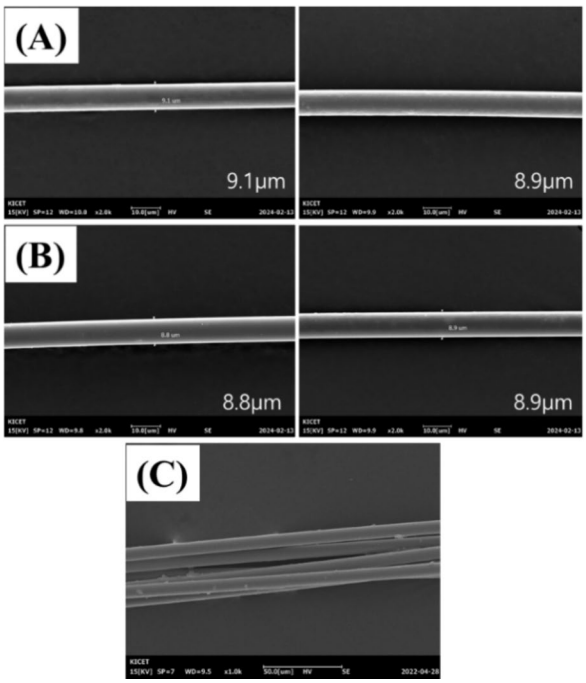

Fig. 9. SEM images of the (**A**) GDMC-Si59 and (**B**) GDMC-La0.2 glass fibers, and (**C**) GDMC-Si59 glass fibers in the fiber strand.

spinning speed of 500 rpm. Note that the fiber tension was adjusted by controlling the spinning speed. The fiber strand with a total length of 25 km and diameter of about 10 μm was obtained (Fig. 8(E)).

The surface of the drawn fibers was examined using the scanning electron microscope (COXEM, EM-30 N). Figure 9(A) and (B) display the SEM images of the GDMC-Si59 and the GDMC-La0.2 glass fibers at the different sections. The fibers of the both glasses showed smooth surfaces at all the sections and the fiber diameter was determined by averaging the measured diameters obtained from various fiber samples at different sections. The average fiber diameter of the both the GDMC-Si59 and the GDMC-La0.2 fiber samples was 9±0.1 μm. Figure 9(C) shows the SEM image of the glass fibers in the fiber strand. As can be seen from the image, it should be noted that the glass fibers in the fiber strand exhibited a smooth surface without any wrinkles.

Since glass fiber strands are used as a reinforcing element for composite structures, mechanical properties of tensile strength and elastic modulus were measured[24–27]. A fiber from the GDMC-Si59 and the GDMC-La0.2

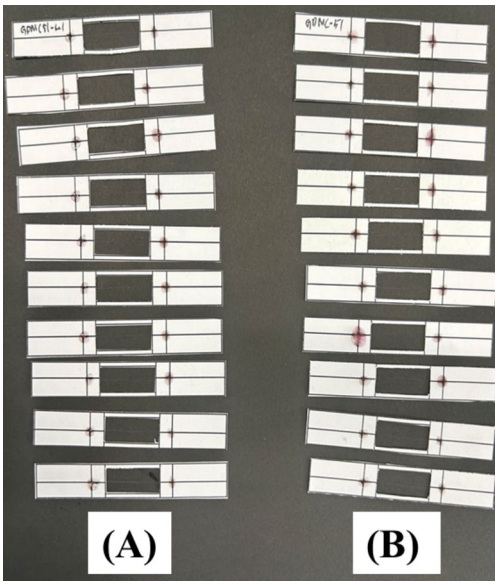

Fig. 10. Photographs of the (**A**) GDMC-Si59 and (**B**) GDMC-La0.2 fibers attached to the paper frames for the mechanical test.

fibers with a length of 20 mm was attached to the paper frames using adhesive as shown in Fig. 10 and tensile tests were conducted using the universal testing machine (INSTRON 5544, 2712-013, USA) equipped with a load cell of 10 N at 0.5 mm/min. Measurements were made with 10 samples of each fiber to obtain a representative set of results. The average tensile strengths were found to be 1.886 and 1.982 GPa for the GDMC-Si59 and the GDMC-La0.2 fibers, respectively. The average Young's moduli were found to be 46.847 and 45.492 GPa for the GDMC-Si59 and the GDMC-La0.2 fibers, respectively. The increase in tensile strength of the GDMC-La0.2 fiber with the addition of La_2O_3 may be attributed to the higher cation field strength of La^{3+}ions that form stronger La-O bonds in the glass network[6,12,28]. On the other hand, the decrease in Young's modulus of the GDMC-La0.2 fiber sample with the addition of La_2O_3 is caused by an increase of the concentration of three-fold boron, that is BO_3, since the BO_3 units make the structure less densely packed even in low boron-containing glasses. This agrees well with the early findings that E- and ECR-glass fibers have higher Young's modulus than that of the new D-glass fibers having high content of B_2O_3[25]. The increase of three-fold BO_3 units in the GDMC glasses with the addition of La_2O_3 was confirmed from the structural analysis (see Fig. 2(B)).

Conclusions

We fabricated two series of alkali-free aluminoborosilicate glasses without and with La_2O_3 by the melt-quenching method. With the additions of SiO_2 and La_2O_3 in the alkali-free aluminoborosilicate glass system, the decrease of the T_g and the increase of the CTE were found, which is due to the depolymerization of the glass network confirmed by the FTIR analysis. Depolymerization of the glass network connectivity with the substitution of SiO_2 for Al_2O_3 in the GDMC-Si glass system is due to the decreasing vibrations of the bridging Si−O (Si−O_b) bonds around 1024 cm^{-1} and increasing vibrations of the non-bridging Si−O (Si−O_{nb}) bonds around 899 cm^{-1} (Q^1). The degree of polymerization decreased in the GDMC-La glass system with the substitution of La_2O_3 for Al_2O_3 and MgO because of the dominance of the Si-O_{nb} bonds around 899 cm^{-1} (Q^1).

The glass with the highest SiO_2 content of 62.7 mol% showed lower Dk and Df values of 4.50 and 2.86×10^{-3} in the present glasses. Notably, the Dk and Df values of the present glasses were lower than those of the commercial E-glass (Dk: 6.9, Df: 7.0×10^{-3} at 10 GHz), L-glass (Dk: 4.8, Df: 3.0×10^{-3} at 10 GHz), and NE-glass (Dk: 4.7, Df: 3.5×10^{-3} at 10 GHz). The La^{3+}-doped glasses are attractive for PCB applications as they exhibit lower CTE and dielectric property (Dk & Df) than the alkali-containing glasses which generally provide higher CTE and dielectric property. All the glasses exhibited excellent thermal stability (ΔT) of $\geq$ 224 °C, low softening temperatures of 784–872 °C, and low CTEs of $3.41-4.67\times10^{-6}$/K that are comparable to those of commercial glasses (AGY, L- and E-glasses).

We have successfully drawn 10 µm glass fibers via continuous melting spinning process and their mechanical properties were investigated. The average tensile strengths and Young's moduli were found to be 1.886 and 1.982 GPa; 46.847 and 45.492 GPa for the GDMC-Si59 and GDMC-La0.2 fibers, respectively. The results clearly indicate that the alkali-free aluminoborosilicate glasses/fibers have application potential as reinforcing materials in PCB applications at high frequencies.

Data availability

All data generated or analyzed during this study are included in this published article.

Received: 4 September 2024; Accepted: 8 November 2024

Published online: 12 November 2024

References

1. Li, H., Eng, D., Tang, C. & Westbrook, P. Low dielectric glass fiber development–new printed circuit board base materials. *Glass Technol. Eur. J. Glass Sci. Technol. A*. **54**, 81–85 (2013).
2. Longobardo, A. V., Wallenberger, F. T. & Bingham, P. A. (eds), Chap. 4, Fiberglass and Glass Technology, Springer Science + Business Media, LLC (2010).
3. Astm, D. *Standard Specification for Glass Fiber Strands*pp. 578–500 (ASTM, West Conshohocken, 2000).
4. Wallenberger, F. T. *Advanced Inorganic Fibers: Processes, Structures, Properties, Applications*pp. 129–166 (Kluwer Academic, 2000).
5. Yan, J., Zhang, T., Tao, H., Zhan, H. & Yue, Y. Structure, crystallization, and performances of alkaline-earth boroaluminosilicate sealing glasses for SOFCs. *J. Am. Ceram. Soc.* **00**, 1–11 (2021).
6. Li, S. et al. Dielectric and thermal properties of aluminoborosilicate glasses doped with mixed rare-earth oxides. *J. Non-Cryst Solids*. **556**, 120550 (2021).
7. Huang, S., Li, S., Wu, F. & Yue, Y. Effect of B_2O_3 on structure and Properties of CaO–MgO–B_2O_3–Al_2O_3–SiO_2 glasses. *J. Inorg. Organomet. Polym.* **25**, 816–822 (2015).
8. Han, J. et al. Structure and crystallization behavior of Al containing glasses in the CaO–B_2O_3–SiO_2 system. *RSC Adv.* **7**, 14709–14715 (2017).
9. Chacon, L. C. et al. Glasses for flat panel displays. *US Patent Application* **7365038B2**, (2008).
10. Hsiang, H., Chen, C. C. & Yang, S. Y. Structure, crystallization, and dielectric properties of the Al_2O_3 filled CaO–B_2O_3–SiO_2–Al_2O_3 glass composites for LTCC applications. *Jpn J. Appl. Phys.* **58**, 091010 (2019).
11. Junfeng, K. et al. Structure, dielectric property and viscosity of alkali-free boroaluminosilicate glasses with the substitution of Al_2O_3 for SiO_2. *J. Non-Cryst Solids*. **537**, 120022 (2020).
12. Zhang, L. et al. Influence of rare earth oxides on structure, dielectric properties and viscosity of alkali-free aluminoborosilicate glasses. *J. Non-Cryst Solids*. **532**, 119886 (2020).
13. Jolivet, V. et al. Quantification of boron in aluminoborosilicate glasses using Raman and ^{11}B NMR. *J. Non-Cryst Solids*. **511**, 50–61 (2019).
14. Bruns, S. et al. Influence of Al_2O_3 addition on structure and mechanical properties of borosilicate glasses. *Front. Mater.* **7**, 189 (2020).
15. Cui, J. et al. The effect of substitution of Al_2O_3 and B_2O_3 for SiO_2 on the properties of cover glass for liquid crystal display: structure, thermal, visco-elastic, and physical properties. *Int. J. Appl. Glass Sci.* **12**, 443–456 (2021).
16. http://www.nittobo.co.jp/business/glassfiber/sp_material/t-glass.htm
17. Boessneck, D. S., Gonterman, J. R. & Prokhorenko, O. A. Low dielectric glass fiber. *US Patent Application*. **2008/0103036**, A1 (2008).
18. Roberts, S. Dielectric constants and polarizabilities of ions in simple crystals and barium titanate. *Phys. Rev.* **76**, 1215–1220 (1949).
19. Dimitrov, V. & Komatsu, T. Correlation among electronegativity, cation polarizability, optical basicity and single bond strength of simple oxides. *J. Solid State Chem.* **196**, 574–578 (2012).
20. Zhao, X., Wang, X., Lin, H. & Wang, Z. Electronic polarizability and optical basicity of lanthanide oxides. *Phys. B.* **392**, 132–136 (2007).
21. Kadathala, L., Park, Y. O., Oh, M. K., Han, W. T. & Kim, B. H. Analysis of the dielectric properties of alkali-free aluminoborosilicate glasses by considering the contributions of electronic and ionic polarizabilities in the GHz frequency range. *Mater*. **17**, 1404 (2024).
22. Cai, L. et al. Glass for 5G applications. *Appl. Phys. Lett.* **119**, 082901 (2021).
23. Kanehara, K., Urata, S., Yasuhara, S., Tsurumi, T. & Hoshina, T. Dielectric property and polarization mechanism of sodium silicate glass in GHz–THz range. *Jpn J. Appl. Phys.* **61**, SN1001 (2022).
24. Korwin-Edson, M. L., Hofmann, D. A. & McGinnis, P. B. Strength of high performance glass reinforcement fiber. *Int. J. Appl. Glass Sci.* **3**, 107–121 (2012).
25. Li, H., Charpentier, T., Du, J. & Vennam, S. Composite reinforcement: recent development of continuous glass fibers. *Int. J. Appl. Glass Sci.* **8**, 23–36 (2017).
26. Li, H., Richards, C. & Watson, J. High-performance glass fiber development for composite applications. *Int. J. Appl. Glass Sci.* **5**, 65–81 (2014).
27. Zu et al. Compositional effects on mechanical properties, viscosity, and crystallization of (Li_2O, B_2O_3, MgO)-Al_2O_3-SiO_2 glasses. *J. Alloys Compds*. **728**, 552–563 (2017).
28. Charpentier, T., Ollier, N. & Li, H. RE_2O_3-alkaline earth-aluminosilicate fiber glasses: melt properties, crystallization, and the network structures. *J. Non-Cryst Solids*. **492**, 115–125 (2018).

Acknowledgements

This study was supported by the National R&D programs [NRF-2021M3H4A3A01050367, NRF-2021M3H4A3A01050369, and NRF-2021M3H4A3A01045740] through the National Research Foundation of Korea funded by the Ministry of Science and ICT and the research program (No. 20223030020230) through a grant provided by the Ministry of Trade, Industry and Energy, Korea. The FTIR spectra of the glass samples in this study were measured at the GIST Advanced Institute of Instrumental Analysis (GAIA), GIST.

Author contributions

L.K. conceptualized the research, analyzed the data, and wrote the original manuscript. Y.-O.P. performed the experiments and characterization. J.H.K., J.-S.L. and Y.H.K. conducted the fiber drawing experiment and post-processing of the SEM and mechanical data of the fiber. J.C.W., W.-T.H. and B.H.K. conceptualized the research, reviewed and edited the manuscript, and supervised the study. All authors reviewed the manuscript.

Declarations

Competing interests

The authors declare no competing interests.

Additional information

Correspondence and requests for materials should be addressed to B.H.K.